On cutting force coefficient model with respect to tool geometry and tool wear

Petr Kolar[1*], Petr Fojtu[1] and Tony Schmitz[2]
[1]*Czech Technical University in Prague, Research Center of Manufacturing Technology, Prague, Czech Republic*
[2]*Center for Precision Metrology, University of North Carolina at Charlotte, Charlotte, USA*
p. kolar@rcmt.cvut.cz, p.fojtu@rcmt.cvut.cz, tony.schmitz@uncc.edu

Abstract

Cutting force models are important for machining processes simulations. This paper presents measurement of cutting forces during C45 (1.0503) carbon steel machining using a coated carbide tool. Various cutting edge geometries and cutting conditions as well as various tool flank wear values were tested. The cutting force coefficients were computed from the experimental data. The results showed that the absolute value of the cutting force coefficients depended on the cutting edge geometry, cutting conditions and tool wear. Additionally, the relative increase in the cutting force coefficients during the tool lifetime was linear and independent of the cutting edge geometries and cutting conditions. The cutting force coefficient models with and without cross components were identified using the linear regression method. Comparison of both models is discussed in the paper.

Keywords: Cutting edge geometry, flank wear, coated carbide tool, cutting force coefficients, linear regression.

1 Introduction

Current machining simulations focus on a comprehensive description of the process–workpiece–machine tool interactions. The core of the simulation is computation of the cutting forces in the time domain during the workpiece material removal. These complex models are based on identified cutting force models.

In general, the cutting force can be described using chip thickness and depth of cut. Cutting force dependence on the undeformed chip cross-section as the main element in the milling process was presented during the 1940s (Martellotti, 1941 and 1945). The relation between the cutting force and the chip cross-section is described with cutting force coefficients. These coefficients are dependent on chip thickness (Kienzle, 1952) as well as on other cutting tool parameters and cutting conditions. The method for tangential, radial and axial cutting force coefficient expression as functions of axial depth of cut and feed per tooth was presented by (Sabberwal, 1962). Mechanistic models (Fu, 1984; Spiewak, 1995) were developed for identification of the cutting force coefficients from experimental data. Computation of the cutting forces from an orthogonal cutting database was presented for elimination of the need for the experimental calibration of each milling cutter geometry for the mechanistic approach (Budak, 1996). This model was generalized for basic machining operations (Kaymakci, 2012).

Tool wear is another important parameter increasing cutting forces. A change in cutting force with relation to the tool wear during turning operations was described in (Oraby, 1991). Teitenberg

* Corresponding author

(Teitenberg, 1992) computed tangential cutting force coefficients for turning operations as a function of feed rate, depth of cut and tool wear. Lin (Lin, 1995) developed a tangential and radial cutting force coefficient model for face milling with respect to cutting conditions and flank wear size. Average chip thickness, average cutting edge length, and flank tool wear were used for the model. The mechanistic model was identified for single cutting edge geometry only. The model was later expanded to include the influence of average cutting tooth number and used for tool flank wear detection during machining (Lin, 1996).

This paper focuses on cutting force coefficient modeling including the effect of cutting edge geometry and tool wear. The flank wear influence is taken into account in the same way as in (Lin, 1995). The ratio between the radial and the tangential cutting force coefficients changing with the flank wear is discussed in more detail. The model also involves the influence of the cutting tool edge geometry (rake angle, clearance angle, helix angle). The paper is organized as follows. The experiments are described in section 2. The experiment results are presented and discussed in section 3. Cutting force coefficient modeling using linear regression is described in section 4. The model results are compared with the measured data.

2 Experiment setup and procedure

The presented results are based on experiments. The main goal of the experiments was to measure the cutting forces for slot milling using shank cutters with various cutting geometries and conditions. Various wear levels were also considered.

2.1 Experiment setup

The experiment setup is shown in Figure 1. The cutting tool was clamped in the spindle of the vertical three axis milling machine. The tool tip zero position was checked with a tachoprobe. A reflection mark was fit with the tool tip in order to get one position signal per every tool revolution. The angular position of the tool tip was gained computationally having 360° between every tachoprobe signal. The machined material was clamped on the Kistler 9255B dynamometer for cutting force measurement. The dynamometer signal was synchronized with the tachoprobe signal. A block of the C45 ((1.0503) carbon steel was used for the cutting force measurement. The same material was cut after every cutting force measurement step to increase tool flank wear.

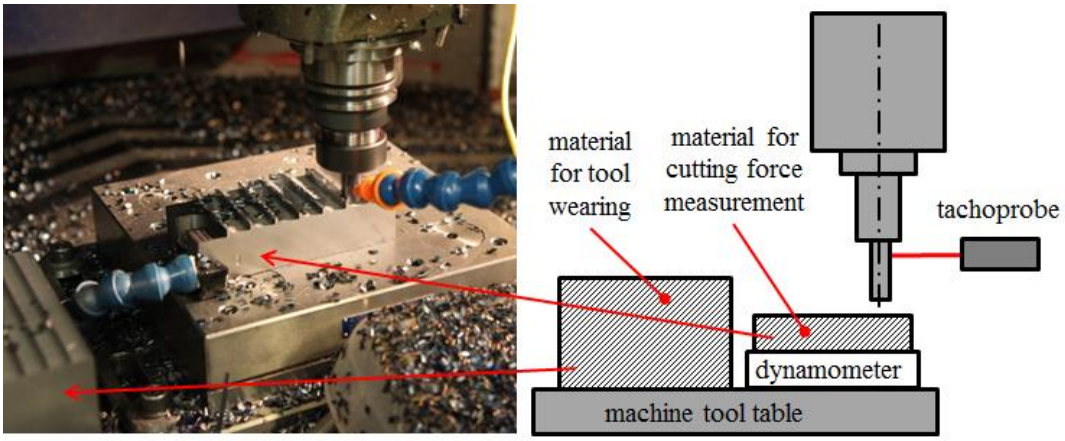

Figure 1: Experiment setup

Rake angle:	γ = 12°, 8°, 4°	Monolithic one-tooth tool; 18 combinations of the cutting edge geometry in total
Clearance angle:	α = 9°, 6°, 3°	
Helix angle:	λ = 25°, 45°	

Table 1: Overview of the cutting edge geometry of the experimental shank cutters.

Cutting speed:	v_c = 80 and 105 m/min	10 combinations of cutting conditions in total
Feed per tooth:	f_z = 0.025, 0.040, 0.055, 0.070, and 0.085 mm	
Depth of cut:	Axial depth: a_p = 4 mm; slot milling	

Table 2: Cutting conditions used for the experiment

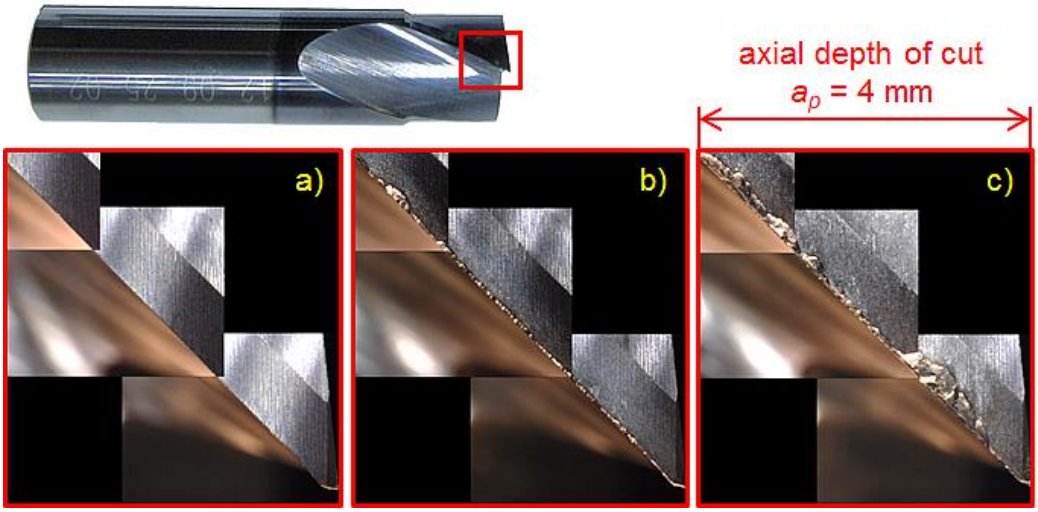

Figure 2: Example of an experimental one-tooth milling cutter and three tool wear levels: a) new tool without flank wear; b) flank wear after 55 minutes of machining; c) flank wear after 111 minutes of machining. The presented example is the cutter with a helix angle of 45°. The engaged cutting edge length is shown. The figures are composed of three photographs for higher depth of field.

The average flank wear value was determined using measurement of the flank wear area on the photograph of the tool. The tested cutting tool was aligned using a specific fixture to have the same tool edge and tool tip position each time. The area of the flank wear was measured with respect to the position of the original cutting edge on the new tool. The resolution of the method was 470 pixels per 1 mm. The measured area was divided by cutting edge length to gain average flank wear value. This procedure also minimizes the influence of local flank wear measurement deviations.

2.2 Experiment procedure

The standard experiment procedure consisted of the following steps.

1. Preparation phase: The raw material was aligned. The cutting tool was clamped and aligned with the tachoprobe.
2. First measurement: Two slots in two directions were cut using the new tool without wear. Combinations of two cutting speed levels and five feed per tooth levels were applied during each slot machining pass. The cutting forces in the stationary coordinate system X, Y, Z were measured with the dynamometer.
3. Repetition of the routine: The block of material next to the dynamometer was machined in order to set a non-zero tool wear level. The defined material volume was removed. The tool flank wear

was measured. Next, two slots were again cut in the material placed on the dynamometer. The cutting forces in the stationary coordinate system were measured again. The cutting speed of 135 m/min and feed per tooth of 0.055 mm were used for wearing of the tool. These cutting conditions caused an increase in the tool flank wear without any undesirable effects such as oxidation crater, edge breakage, etc. The flank wear was measured along the cutting edge. The maximum and average flank wear values were recorded. An example of the worn tool is provided in Figure 2.

4. The test finished when the tool reached the defined maximum flank wear of 300 μm.

3 Experiment results

3.1 Statistical quality check of the experimental data

The main results of the experiment were the measured stationary cutting forces F_X, F_Y, F_Z. These results were determined for all combinations of cutting tool geometry and cutting conditions. There are four result sets for each combination mentioned: two result sets from two slot cuts and one experiment repetition.

The procedure provided a full factorial experiment. The active force (cutting force in the cut plane) was evaluated as a characteristic parameter of each data set:

$$F_A = \sqrt{F_X^2 + F_Y^2} \tag{1}$$

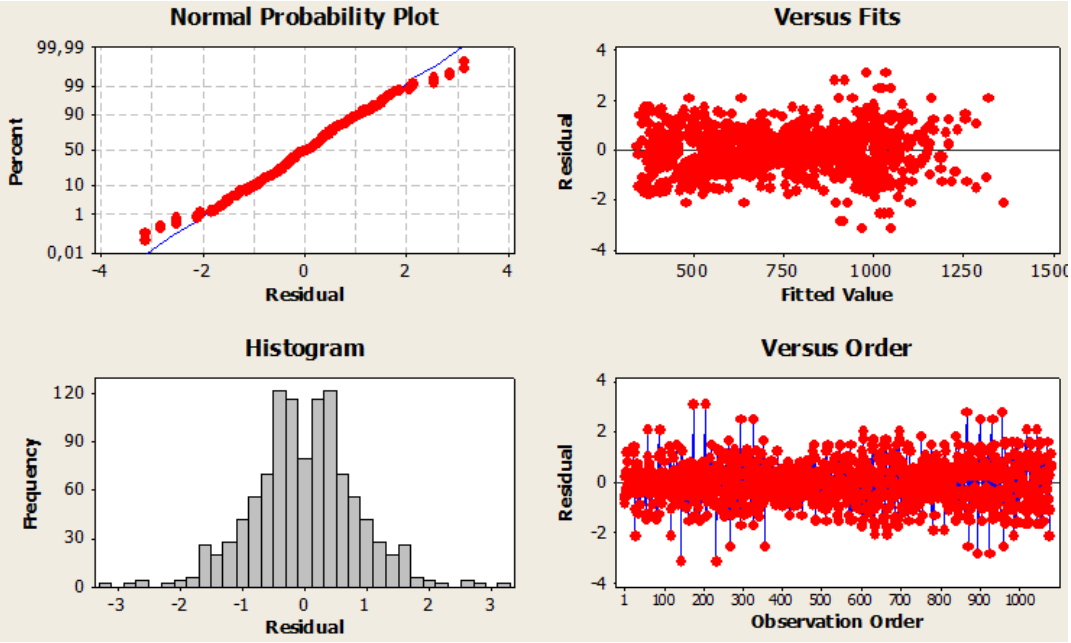

Figure 3: Residual plots for active cutting force F_A.

Statistical quality check is presented in Figure 3. Normal probability plot shows that residues are deviated non-significantly. The distribution in the histogram shows neither any skewness nor kurtosis. The data seems to be mirrored but it is close to the normal distribution. The reason for mirroring could lie in the usage of interaction order during data evaluation. As can be seen in the residual vs. fits diagram, the data does not show any significant deviation from expected values. No increase in the residuum values is visible in the residual vs. order graph. The time effect of the measurement is not visible.

The ANOVA method was used for a preliminary evaluation of the data. The sensitivity analysis is presented in Figure 4. As can be seen, the active force is strongly sensitive to feed per tooth and tool wear values. There is moderate sensitivity to the rake angle and helix angle value. There is low sensitivity to clearance angle and to cutting speed. Low sensitivity to cutting speed is due to the small range of cutting speed tested. The results correlate very well with classical cutting mechanics. The sensitivity analysis shows an impact of the presented input parameters on the cutting force value. Chip thickness has a significant influence as can be seen in the feed per tooth diagram. The central importance of the rake angle, which directly influences the chip formation processes, can be seen in the active cutting force results. The clearance angle, which influences the friction process on the tool flank, is not important. However, the flank wear also influences the local values of the rake angle. Therefore, the flank wear seems to be as important as tool rake geometry.

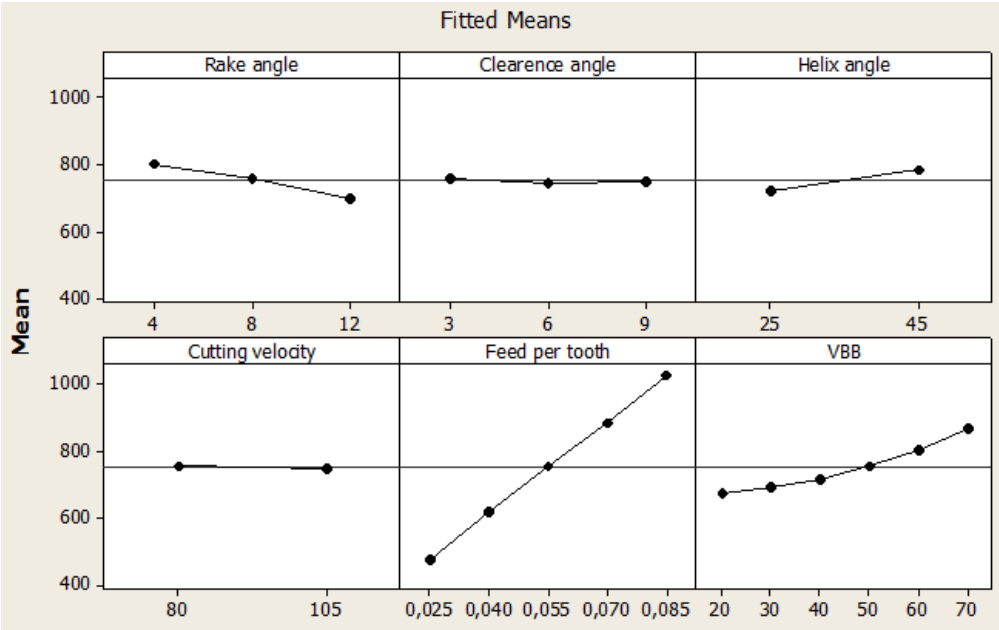

Figure 4: Sensitivity of active force F_A to cutting edge geometry and cutting conditions.

3.2 Tool wear results

The tool wear values are presented in Figure 5. Maximum and mean flank wear values were computed from measured data sets as was described in section 2.1. The flank wear is plotted for various cutting edge geometry (rake angle γ – clearance angle α) and two helix angles (λ = 25° and 45°) (Figure 5). In some cases, the curves do not show the typical shape with intensive wear at the beginning and the end of the tool life time. This is because the time step was too coarse for identification of the initial tool flank wear. The important fact is that the flank wear mean value was increasing gradually. The goal of the experiment was the cutting force measurement for a specific flank wear value. As can be seen, the tool life time was in the range from 70 to 140 minutes with respect to the specific tool cutting edge geometry. The flank wear had similar mean value for various helix angles and machining time. The cutting forces were measured for all tool geometries at all specific flank wear values.

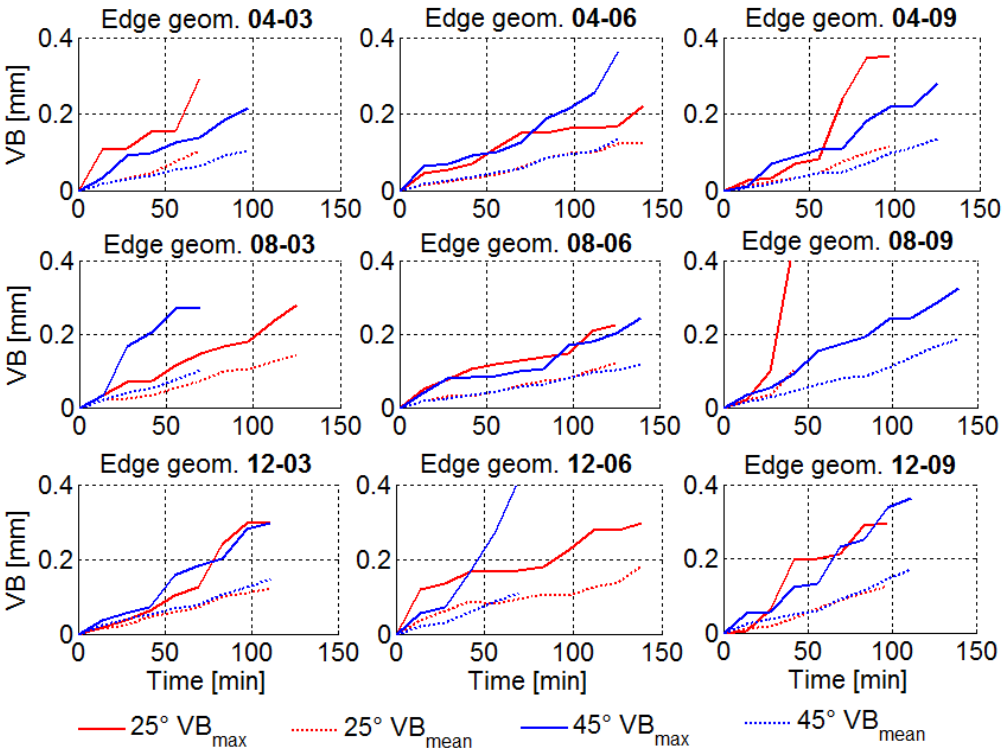

Figure 5: Maximum and mean flank wear for various cutting edge geometry (rake angle γ – clearance angle α) and two helix angles (λ = 25° and 45°). Results were achieved for these cutting conditions: cutting speed of 135 m/min and feed per tooth of 0.055 mm.

3.3 Geometrical model of tool tooth engagement

The machining tests (slot milling) were done in the +Y direction; see Figure 6. A simplified circular movement of the tool tip was used for a subsequent model.

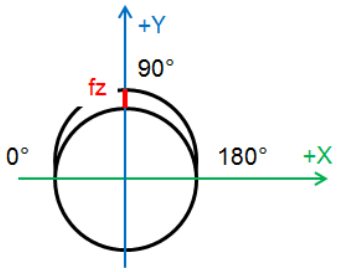

Figure 6: Machine axes orientation during the experiment.

The experimental data were measured in the stationary machine tool coordinate system X, Y, Z. This data was transformed to the rotational tool coordinate system: tangential – radial – axial. A geometrical model used for this transformation is shown in Figure 7. The tool tip position was described by the angle ϕ. The angular length of the cutting edge engagement ϕ_Z was dependent on the helix angle λ and the axial depth of the cut a_p. The angular length of the cutting edge engagement ϕ_Z was the difference between the tooth engagement start angle ϕ_S and tooth engagement end angle ϕ_E. The tooth engagement start angle ϕ_S was identical with the tool tip position angle ϕ in the region of $\phi \in <0°, 180°>$. The tool tooth removed a chip with the thickness of a_p from the workpiece. The maximum chip thickness was equal to feed per tooth ratio f_z in the position ϕ = 90°. The area of the tool rake face was inclined by helix angle λ (the blue area in Figure 7). All cutting forces acted continuously on this area, i.e. stationary cutting forces F_X, F_Y, F_Z and also rotating cutting forces F_C, F_R, F_{AX}. In this model, all forces were represented by their resultant force acting at the

centroid of the inclined area. The angular position of this centroid is described with angle ϕ_T. The following assumptions are valid for this model:

- Forces F_X and F_Y are perpendicular to each other. The active force F_A is a resultant force of these two forces.
- A line between the centroid of the inclined area and the tool center (axis of the tool rotation) defines the direction of the radial force F_R. The size of the radial force F_R is a projection of the active force F_A into this radial direction.
- The active force inclination angle β is defined between the radial force direction and the active force direction.
- The tangential direction is perpendicular to the defined radial direction. The size of the tangential force F_C is a projection of the active force F_A into this tangential direction.

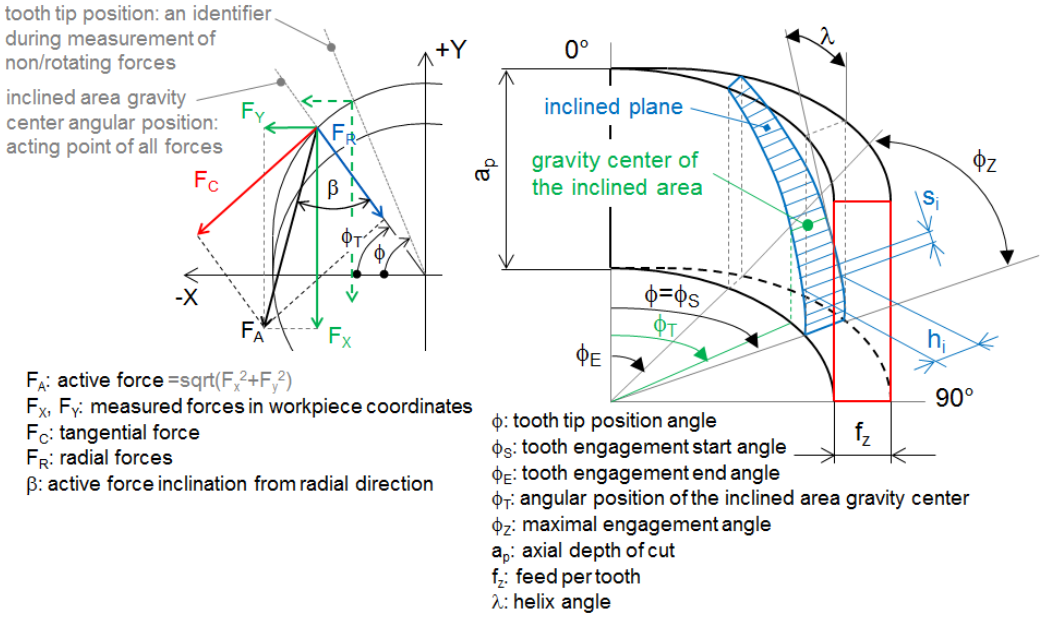

Figure 7: Geometric model of the tool tooth engagement.

It is possible to calculate the tangential, radial and axial rotating cutting forces F_C, F_R, F_{AX} from the stationary cutting forces F_X, F_Y, F_Z using this geometric model for each tool tip position ϕ. The inclined cut area and also engaged cutting edge length is divided into n segments along the Z axis. The angular start position of each segment ϕ_i is calculated for each tool tip position ϕ. The size of the contact area A_i (the blue inclined plane) can be computed in each tool tip position ϕ:

$$A_i = \sum_{1}^{n} s_i \cdot h_i \tag{2}$$

where s_i is length of the cutting edge length segment and h_i is relevant chip thickness in each ϕ_i position. The angular position of the inclined area centroid ϕ_T is computed as:

$$\phi_T = \frac{\sum_{1}^{n} s_i \cdot h_i \cdot \phi_i}{\sum_{1}^{n} s_i \cdot h_i} \tag{3}$$

The cutting force coefficients can be computed as a ratio of the cutting force and the cut area:

$$k_C = \frac{F_C}{A_i};\ k_R = \frac{F_R}{A_i};\ k_{AX} = \frac{F_{AX}}{A_i} \tag{4}$$

This procedure enables the computation of the coefficients and their dependence on cutting geometry, tool wear, cutting conditions and tool tip position for each experimental data set:

$$k_C, k_R, k_{AX} = \text{function of } (\gamma, \alpha, \lambda, VB_{av}, v_c, f_z, \phi) \tag{5}$$

The procedure is demonstrated on the example in Figure 8. The tool tip position was detected with the tachoprobe (see section 2.1). The measured and computed forces in the stationary machine tool coordinate system and the rotating tool coordinate system are shown. The gray border of the measured F_X, F_Y, F_Z forces are the real measured data. The fitted curve (color solid line) is used for subsequent computations. The cutting edge full engagement is marked. The size of this zone is dependent on the helix angle and axial depth of cut.

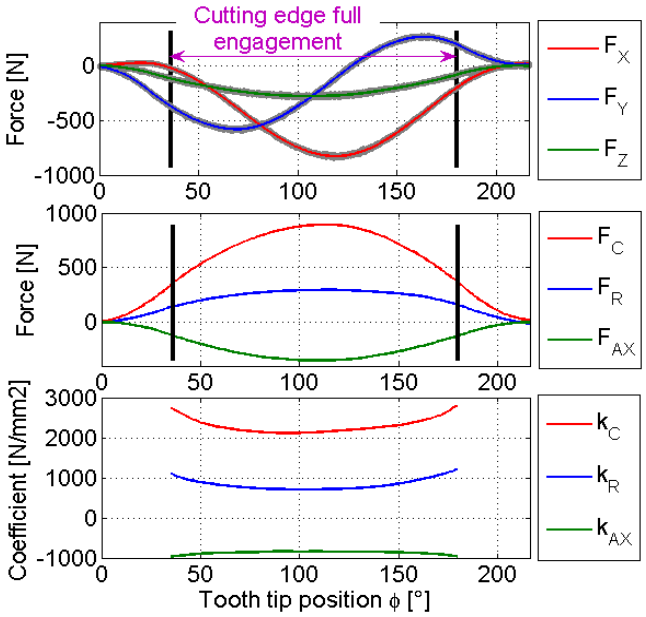

Figure 8: Example of measured and computed data for the tool with cutting edge geometry: $\gamma = 4°$, $\alpha = 6°$, $\lambda = 45°$; cutting conditions: $f_z = 0.085$ mm, $v_c = 80$ m/min, new tool (no wear).

An example of the computed cutting force coefficients dependent on tool tip position is provided in Figure 8. The measured stationary cutting forces are shown in the top left-hand corner and the computed rotating cutting forces in the bottom left-hand corner. The computed cutting force coefficients are plotted in the top right-hand corner. The results are plotted for fully engaged cutting edge area as the chip thickness is small and the cut is not clearly defined especially at the beginning and end of the cut. As can be seen, the cutting force coefficients are minimal in the area of maximum chip thickness (tool tip position about 100°). The coefficients are maximal at the start and end of the cut, where the chip thickness is smaller. This conforms to the Kienzle law (Kienzle, 1952).

3.4 Discussion of cutting force coefficient changes

As presented in section 3.1, the cutting force coefficients are sensitive to tool wear, feed per tooth value and cutting edge geometry. The tangential cutting force coefficients k_C and the radial cutting force coefficients k_R for various flank wear value and cutting edge geometry are plotted below as an example.

The first case for a tool with the cutting edge geometry of $\gamma = 12°$, $\alpha = 6°$, $\lambda = 25°$ is an example of a tool with a long life time (up to 140 minutes). The flank wear value increases during the tool life time. The mean value of the tangential cutting force coefficient increases linearly by 37% during the whole tool life time (Figure 9). The mean value of the radial cutting force coefficient increases linearly by 152% during the whole tool life time.

The second case, the tool with the cutting edge geometry of $\gamma = 8°$, $\alpha = 3°$, $\lambda = 45°$, is an example of a tool with a shorter life time (approx. 70 minutes). The abrasion of this tool's cutting edge is more

intensive due to very positive geometry. The flank wear value increases during the tool life time. The mean value of the tangential cutting force coefficient increases linearly by 32% during the whole tool life time (Figure 10). The mean value of the radial cutting force coefficient increases linearly by 150% during the whole tool life time.

The average value of the cutting force coefficient increase was computed from the result group of tools with various rake angles, clearance angles and cutting conditions for a specific helix angle and cutting speed. As can be seen in Table 3, the tangential cutting force coefficient increases by approximately 42% during the whole life time of all tested tools. This value has also a small standard deviation of 11%. The radial cutting force coefficient increases by approximately 200% during the whole life time of all tested tools, see Table 4. Dependence on the helix angle visible in the table is not significant because standard deviation of results is about 70%. The general result is that the radial cutting forces increase more intensively than tangential cutting forces with increased tool wear.

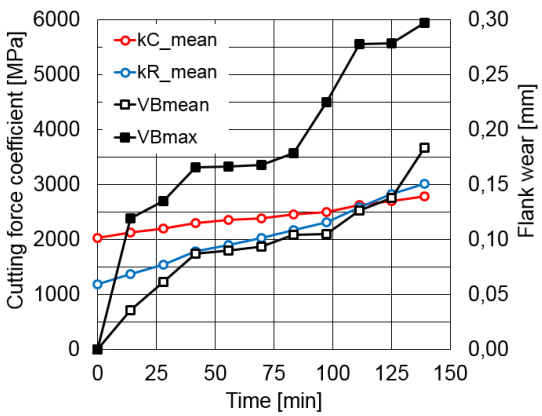

Figure 9: Tangential and radial cutting coefficient change with respect to tool wear for the tool with the cutting edge geometry: γ = 12°, α = 6°, λ = 25°

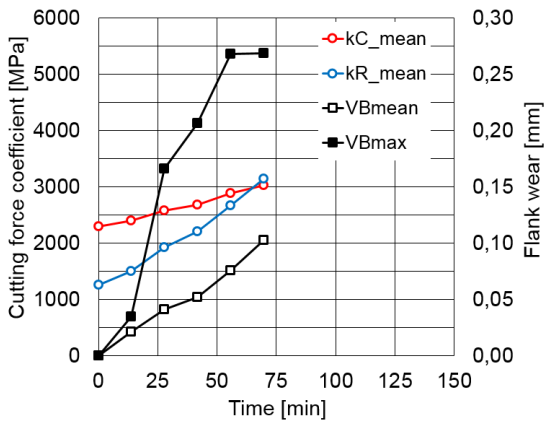

Figure 10: Tangential and radial cutting coefficient change with respect to tool wear for the tool with the cutting edge geometry: γ = 8°, α = 3°, λ = 45°

Δk_C		Helix angle λ	
		25°	45°
Cutting speed v_c	80 m/min	41%	46%
	105 m/min	36%	46%

Table 3: Average increasing of the tangential cutting force coefficient during tool life time.

Δk_R		Helix angle λ	
		25°	45°
Cutting speed v_c	80 m/min	175%	212%
	105 m/min	174%	237%

Table 4: Average increasing of the radial cutting force coefficient during tool life time.

4 Cutting force coefficient model

As shown in the previous section, the cutting force coefficients depend on cutting edge geometry, cutting conditions (including chip thickness dependent on the tool tooth angular position during the workpiece cutting), and also on tool wear. It follows that there are seven independent input parameters for the model (Table 6). The linear regression method was used for the identification of parameters. Full tooth engagement area was used for the identification. Identification with cross components (i.e. combination of input parameters) and without cross components (i.e. without combination of input parameters possible) was done.

4.1 Model parameter identification with cross components

The mathematic approximation of all input parameters and their combinations using the linear regression method was performed. The dependence on the cutting speed was assumed as linear. Other parameters and their combinations could be described by polynomic functions up to third order. The input conditions for the linear regression were as follows: $\boldsymbol{I}$ is multi index vector: $\boldsymbol{I} = (i_1, i_2, \ldots, i_n)$; $\boldsymbol{\Omega}$ is a combination vector of indeces: $\boldsymbol{\Omega}$ = {all combinations of {1,1,1,2,2,2,3,3,3,4,4,4,5,5,5,6,7,7,7}}

$$f = \sum_{I \in \Omega} a_i \prod_{j=i} x_j \tag{6}$$

This regression definition enabled us to identify 1152 parameter combinations. The highest R^2 parameter values for the tangential, radial and axial cutting force coefficients were achieved for 410 identified non-zero constants and input parameter combinations. The identified parameter order for the input parameters is shown in Table 6. A large number of identified parameters are a result of the mathematical analysis. Physical representation of parameter combinations (cross components) and their orders is not clear. An example of the model result for one selected tool type and specific cutting conditions can be seen in Figure 11. As can be seen, the identified model follows the experimental data with the error lower than 5%. The quality of the model is also demonstrated by a high R^2 value of 90%.

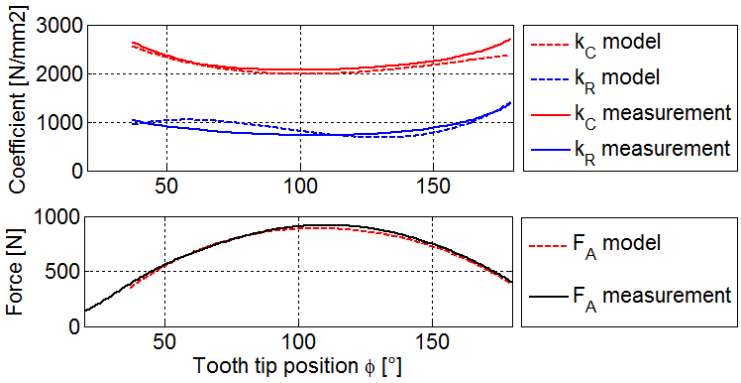

Figure 11: Comparison of the identified model result and experiment result. Presented example: cutting edge geometry: γ = 4°, α = 9°, λ = 45°; cutting parameters: f_z = 0.085 mm, v_c = 105 m/min.

4.2 Model parameter identification without cross components

The mathematic approximation of all input parameters without their combinations using the linear regression method was done in the second step. The model without cross components was used for easier physical representation of the results. The model was identified with first order of all parameters and also with second order of ϕ, γ, f_z and VB_{mean} parameters. These selected higher orders follow the importance of the mentioned parameters identified in section 3.1. The cutting force coefficient model has this form:

$$\begin{aligned} k_{C,R} = {} & a_{0C,R} + a_{1C,R} \cdot \phi_T + a_{2C,R} \cdot \phi_T^2 + a_{3C,R} \cdot \gamma + a_{4C,R} \cdot \gamma^2 + a_{5C,R} \cdot \alpha + a_{6C,R} \cdot \lambda + \\ & + a_{7C,R} \cdot f_Z + a_{8C,R} \cdot f_Z^2 + a_{9C,R} \cdot vc + a_{10C,R} \cdot VB_{mean} + a_{11C,R} \cdot VB_{mean}^2 \end{aligned} \tag{7}$$

Parameter ϕ_T is used in the model because the mean chip thickness as an important factor is dependent on the following parameter:

$$h_\phi = f_Z \cdot \sin \phi_T \tag{8}$$

The parameter ϕ_T can be computed for every ϕ_i position using (3). The identified model coefficients are shown in Table 5. As can be seen in Table 6, the full linear model has low R^2 values of approximately 53%. The non-linear model with four quadratic parameters has a higher R^2 value of approximately 70-75%. An example of the computed cutting force coefficients and also a comparison of the active force (1) computed using the described model with the measured data is presented in Figure 12. As can be seen, the model approximation is not good. Results are discussed in the next section.

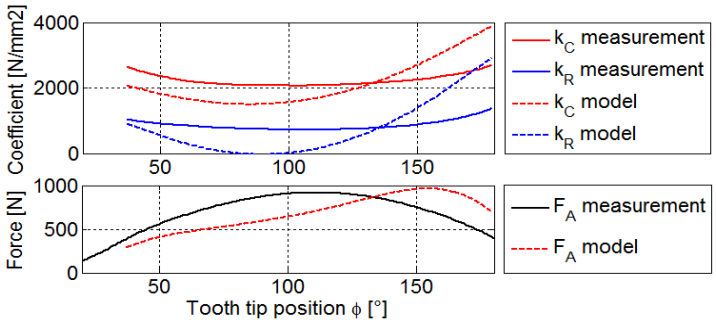

Figure 12: Comparison of the identified model result and experiment result. Presented example: cutting edge geometry: $\gamma = 4°$, $\alpha = 9°$, $\lambda = 45°$; cutting parameters: $f_z = 0.085$ mm, $v_c = 105$ m/min.

Input parameter	Parameter coefficient	k_C linear model	k_R linear model	k_C nonlinear model	k_R nonlinear model
ϕ_T	a_1	12.217	12,869	-41.197	-60.068
ϕ_T^2	a_2	0	0	0.309	0.422
γ	a_3	-39.655	-51,890	-144.348	-1.826
γ^2	a_4	0	0	6.587	-3.110
α	a_5	7.362	-27,290	7.433	-28.802
λ	a_6	18.917	4,799	27.622	17.661
f_z	a_7	-20672.289	-30570,015	-57278.622	-81567.134
f_z^2	a_8	0	0	332784.846	463610.167
v_c	a_9	-2.751	5,304	-2.751	5.304
VB_{mean}	a_{10}	12.331	29,492	11.703	16.064
VB_{mean}^2	a_{11}	0	0	0.00576	0.118
constant	a_0	2129.861	1435,174	4784.571	4656.180

Table 5: Results of the linear regression model without cross components

4.3 Model discussion

Two types of models were identified using linear regression from the experimental data. As a result of the general mathematical analysis, the first non-linear model with cross components was composed of 410 components. The R^2 value is about 90% (see Table 6). However, the physical interpretation of these components and also significance of each component is not clear. If a non-linear model without cross components is used, the R^2 value is about 75%. The model would be able to compute mean values of the cutting forces. If force dependence on the tool tip position is observed, the model has deviations of approximately 20%. Comparing both results, it is possible to say that cross components are important for a comprehensive description of the cutting force coefficient model depending on the tool geometry, cutting conditions and tool wear. A detailed analysis of the significance of each component should be done in further research.

ID	Parameter description:	Identification with cross components	Identification without cross components	
1	ϕ (tooth tip angular position)	cubic	quadratic	linear
2	γ (rake angle)	quadratic	quadratic	linear
3	α (clearance angle)	quadratic	linear	linear
4	λ (helix angle)	linear	linear	linear
5	f_z (feed per tooth)	cubic	quadratic	linear
6	v_c (cutting speed)	linear	linear	linear
7	VB_{mean} (flank wear mean value)	linear	quadratic	linear
	R^2 values:	k_C: 90%; k_R: 91%	k_C: 76%; k_R: 70%	k_C: 53%; k_R: 53%

Table 6: Identified parameter order for the input parameters and resulting R^2 values

5 Summary and conclusion

The series of experiments were done for measurement of cutting forces during carbon steel milling using tools with various cutting edge geometries, cutting conditions and flank wear level. The cutting force coefficients were computed using the kinematic model. Two types of models – with and without cross components – were identified using the linear regression. The results can be summarized in this manner:

- Two sets of specific tools for the experiment were produced using standard technology for monolithic tools. Thus, the results should be applicable to monolithic coated carbide tools and C45 steel machining.
- Experiment observations show that the radial cutting force coefficient increases more intensively than the tangential radial force coefficient. Relative increasing of both coefficients during tool life is similar for all tested cutting edge geometries. Although the flank wear is non-linear during the tool life time, the relative increasing of the cutting force coefficients is linear.
- Although the ANOVA analysis shows independent model input, cutting force coefficient model identifications using the linear regression of the experimental data show importance of the cross components in the model. Identification of proper parameter combination should be the subject of further research.
- Partial model results are similar as in published work (Lin, 1995; Budak, 1996). The added advantage of this approach is that the identified models involve the full cutting edge geometry (rake angle, clearance angle, helix angle), cutting conditions (cutting speed, feed per tooth) and also cutting force change due to tool wear.

Acknowledgement

The research leading to these results has been funded by the Czech Ministry of Education, Youth and Sport under grant project No. LH12065.

References

Martellotti ME. An analysis of the milling process. *Transactions of ASME* 1941; 63: 677.

Martellotti ME. An analysis of the milling process II. Down milling. *Transactions of ASME 1945*; 67: 233.

Kienzle O. Die Bestimmung von Kräften und Leistungen an spanenden Werkzeugen und Werkzeugmaschinen. In: *Zeitschrift des Vereins deutscher Ingenieure*, 1952, pp. 657–662.

Sabberwal AJP. Cutting forces in down milling. *International Journal of Machine Tool Design and Research* 1962; 2: 27-41.

Fu HJ, DeVor RE and Kapoor SG. A mechanistic model for the prediction of the force system in face milling operations. *Journal of Manufacturing Science and Engineering* 1984; 106(1): 81-88.

Oraby SE and Hayhurst DR. Development of models for tool wear force relationships in metal cutting. *International Journal of Mechanical Sciences* 1991; 33(2): 125-138.

Teitenberg TM, Bayoumi AE and Yucesan G. Tool wear modeling through an analytic mechanistic model of milling processes. *Wear* 1992; 154(2): 287–304.

Lin SC and Yang RJ. Force-based model for tool wear monitoring in face milling. *International Journal of Machine Tools and Manufacture* 1995; 35(9): 1201-1211.

Spiewak S. An improved model of the chip thickness in milling. *Annals of the CIRP* 1995; 44(1): 39–42.

Budak E, Altintas Y and Armarego E. Prediction of milling force coefficients from orthogonal cutting data. *Journal of Manufacturing Science and Engineering* 1996; 118(2): 216-224.

Lin SC and Lin RJ. Tool wear monitoring in face milling using force signals. *Wear* 1996; 198: 136-142.

Kaymakci M, Kilic ZM and Altintas Y. Unified cutting force model for turning, boring, drilling and milling operations. *International Journal of Machine Tools & Manufacture* 2012; 54–55: 34–45.